Appl. Math. Mech. -Engl. Ed., 2008, **29**(8):1033–1044
DOI 10.1007/s10483-008-0807-x

Applied Mathematics and Mechanics (English Edition)

Enhancement of natural convection heat transfer from a fin by triangular perforation of bases parallel and toward its tip *

Abdullah H. AlEssa[1], Mohamad I. Al-Widyan[2]

(1. Al-Balqa Applied University, Al-Husn University College, Al-Husn, Irbid-Jordan;
2. College of Engineering, Jordan University of Science and Technology,
P. O. Box 3030, Irbid 22110, Jordan)

(Communicated by LIN Jian-zhong)

Abstract This study examines the heat transfer enhancement from a horizontal rectangular fin embedded with triangular perforations (their bases parallel and toward the fin tip) under natural convection. The fin's heat dissipation rate is compared to that of an equivalent solid one. The parameters considered are geometrical dimensions and thermal properties of the fin and the perforations. The gain in the heat transfer enhancement and the fin weight reduction due to the perforations are considered. The study shows that the heat dissipation from the perforated fin for a certain range of triangular perforation dimensions and spaces between perforations result in improvement in the heat transfer over the equivalent solid fin. The heat transfer enhancement of the perforated fin increases as the fin thermal conductivity and its thickness are increased.

Key words finned surfaces, heat transfer enhancement, triangular perforations, natural convection, finite element, perforated fin, heat dissipation

Chinese Library Classification TB131, TB61$^+$1
2000 Mathematics Subject Classification 76E06

Nomenclature

A, cross sectional area of the fin;
A_c, cross sectional area of the perforation;
Bi, Biot number;
b, triangular perforation dimension;
h, heat transfer coefficient;
k, thermal conductivity of fin material;
L, fin length;
$\boldsymbol{l}$, unit vector;
L_c, characteristic length;
N, number of perforations;
Ne, total number of finite elements of the perforated fin;
N_f, number of finite elements in one of the uniform regions (A or C);
N_n, total number of nodes;
N_t, number of finite elements in the tapered region (B);
Nu, average Nusselt number;
Nu_c, average Nusselt number of the inner perforation surface;
OA, open area of the perforated surface;
Q, heat transfer rate;
Ra, Rayleigh number;
Ra_c, Rayleigh number of the perforation inner lining surface;
ROA, ratio of the open area;
RQF, ratio of the heat dissipation rate of the perforated fin to that of the non-perforated fin;

* Received Mar. 13, 2008 / Revised Jun. 10, 2008
Corresponding author Abdullah H. AlEssa, E-mail: abdd104@yahoo.com

RWF, ratio of the perforated fin weight to that of the solid fin (ratio of weight reduction);
S, perforation spacing;
T, temperature;
t, fin thickness;
W, fin width;
W_{pf}, perforated fin weight;
W_{sf}, solid fin weight;

Subscripts and superscripts

b, fin base;
l, lower surface of the fin;
max, maximum;
pc, perforation inner surface (within the perforation);
pf, perforated fin;
ps, perforated surface or the remaining solid portion of the perforated fin;
sf, solid (non-perforated) fin;
ss, solid surface;
t, fin tip;
u, upper surface of fin;
x, longitudinal direction or coordinate;
y, transverse (lateral) direction with the fin width or coordinate;
z, transverse (lateral) direction with the fin thickness or coordinate;
∞, ambient.

Introduction

The removal of excessive heat from system components is essential to avoid the damaging effects of burning or overheating. Therefore, the enhancement of heat transfer is an important subject in thermal engineering. The heat transfer from surfaces may in general be enhanced by increasing the heat transfer coefficient between a surface and its surroundings, by increasing the heat transfer area of the surface, or by both. In most cases, the area of heat transfer is increased by utilizing the extended surfaces in the form of fins attached to walls and surfaces[1]. Fins, as heat transfer enhancement devices, have been quite common. As extended surface technology continues to grow, new design ideas have emerged, including fins made of anisotropic composites, porous media, and interrupted plates[1−3]. Due to the high demand for lightweight, compact, and economical fins, the optimization of the fin size is of great importance. Therefore, fins must be designed to achieve maximum heat removal with minimum material expenditure, taken into account, and also, with the ease of manufacturing the fin shape[4−6]. A large number of studies have been conducted on optimizing fin shapes. Other studies have introduced shape modifications by cutting some materials from fins to make cavities, holes, slots, grooves or channels through the fin body to increase the heat transfer area and/or the heat transfer coefficient[5−8]. One popular heat transfer augmentation technique involves the use of rough or interrupted surfaces of different configurations. The surface roughness or interruption aims at promoting surface turbulence that is mainly intended to increase the heat transfer coefficient rather than the surface area[1,7,9]. It was reported that non-flat surfaces have free convection coefficients that are 50% to 100% more than those of flat surfaces[1,9]. Several researchers reported a similar trend for interrupted, perforated and serrated surfaces, attributing the improvement to the restarting of the thermal boundary layer after each interruption, indicating that the increase in convection coefficient is even more than enough to offset lost areas, if any[1]. Perforated plates (fins) represent an example of surface interruption[1,7−8] and are widely used in different heat exchangers, film cooling, and solar collector applications. Despite the fact that correlations for the convection coefficients within cavities and over the surfaces of non-perforated plates are readily available[1,9−10], literature search indicates a lack of such relations for perforated surfaces under the natural convection. Consequently, in the natural convection, the surface heat transfer coefficients were estimated based on the concepts of the augmentation ratio and the open area ratio[1−2]. In the forced convection, there are many studies dealing with the enhancement of heat transfer as in Refs. [11–12]. In Ref. [11], an experimental study was conducted to investigate the heat transfer and friction loss characteristics of a horizontal rectangular channel with hollow rectangular profile fins attached over one of its heated surfaces. The study showed a significant enhancement of the heat transfer due to the hollow fins. In Ref. [12], another experimental study on the forced heat transfer enhancement over a flat

surface equipped with square cross-sectional perforated pin fins in a rectangular channel was conducted. The experimental results showed that the use of the square pin fins with the circular perforations lead to the heat transfer enhancement.

The main objective of the present study is to investigate the effect of introducing triangular perforations on heat transfer enhancement from a horizontal rectangular fin subjected to natural convection. The modification in this work is the vertically equilateral triangular perforations made through the fin thickness. The study investigates the influence of perforations on the heat transfer rate or the heat dissipation rate of the perforated fin. The modified fin (perforated fin) is compared to a corresponding solid (non-perforated) fin in terms of the heat transfer rate. The study eventually attempts to make the best use of the material and size of a given fin, which involves some sort of optimization. The specific objectives of the work may be summarized as follows: Evaluate the influence of the relevant fin and perforation factors on the enhancement of the heat transfer rate. Then determine the values of parameters that would result in the maximum heat transfer enhancement of the perforated fin compared to the solid counterpart.

1 Assumptions for analysis

The classical treatment of fins, which assumes the one-dimensional heat conduction with small Biot number (less than 0.01), was considered[13−14]. The perforated fin with triangular perforations analyzed in this study is shown in Fig. 1. Figure 2 shows the symmetrical part considered for the heat transfer analysis (shown hatched). For this part of the fin, the transverse Biot number in the z direction Bi_z can be calculated by the expression $Bi_z = h_{\mathrm{pc}} \cdot t/2k$ and the transverse Biot number in the y direction Bi_y can be calculated by $Bi_y = h_{\mathrm{ps}} \cdot (S_y + b/2)/k$. As the values of Bi_z and Bi_y are less than 0.01, the heat transfer in the z and y directions can be assumed lumped, and a one dimension solution can be considered. If the values of Bi_z and Bi_y are greater than 0.01, then the heat transfer solution must be two or three dimensional. In this study, the parameters of the perforated fin are taken as they lead to values of Bi_z and Bi_y smaller than 0.01. The analysis and results reported are based on the following assumptions:

(i) steady and one-dimensional heat conduction,
(ii) homogeneous and isotropic fin material with constant thermal conductivity,
(iii) no heat sources/sinks in the fin body,
(iv) uniform base and ambient temperatures,
(v) side area of the fin is much smaller than its surface area ($w \gg t$),
(vi) uniform heat transfer coefficient over the fin surfaces (perforated or solid),
(vii) negligible radiation effects.

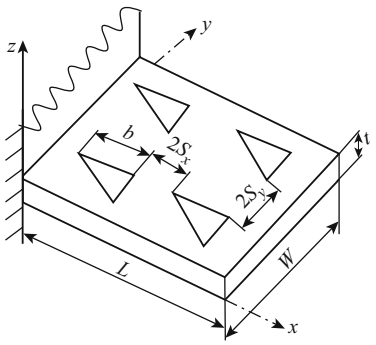

Fig. 1 The fin with equilateral triangular perforations (perforation bases are parallel and toward the fin tip)

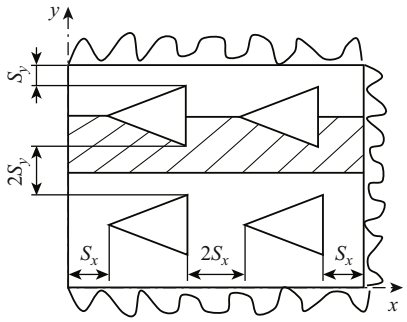

Fig. 2 The symmetrical hatched part used in the mathematical formulation of the perforated fin

2 Heat transfer analysis

Based on the above assumptions, the energy equation of the fin along with the boundary conditions may be stated as follows[15]:

$$k\frac{d^2T}{dx^2} = 0. \tag{1}$$

The associated boundary conditions are:

(i) at the fin base ($x = 0$),

$$T = T_{\mathrm{b}}; \tag{2}$$

(ii) at the perforated surfaces,

$$k\frac{dT}{dx}x + h_{\mathrm{ps}}(T - T_\infty) + h_{\mathrm{pc}}(T - T_\infty) = 0. \tag{3}$$

As shown in Fig. 1, the heat transfer surface area including the tip of the fin with triangular perforations is expressed as

$$\begin{aligned} A_{\mathrm{pf}} &= (2W \times L - 2N_x \times N_y \times A_{\mathrm{c}}) + (W \times t) + (N_x \times N_y \times A_{\mathrm{pc}}) \\ &= A_{\mathrm{f}} + N_x \times N_y(A_{\mathrm{pc}} - 2A_{\mathrm{c}}) \\ &= A_{\mathrm{f}} + N_x \times N_y \times b\Big(3t - b\sin\frac{\pi}{3}/2\Big). \end{aligned} \tag{4}$$

The material weight of the perforated fin is compared to that of the non-perforated one by the weight reduction ratio *RWF*, which is given by

$$\begin{aligned} RWF &= W_{\mathrm{pf}}/W_{\mathrm{sf}} \\ &= (L \times W \times t - N_x \times N_y \times A_{\mathrm{c}} \times t)/(L \times W \times t) \\ &= 1 - (N_x \times N_y \times A_{\mathrm{c}} \times t)/(L \times W \times t) \\ &= 1 - N_x \times N_y \times b^2 \sin\frac{\pi}{3}/(2L \times W). \end{aligned} \tag{5}$$

The numbers of triangular perforations N_x and N_y, which must be integers, in the perforated fin with a given length and width, are obtained from the following expressions:

$$N_x = \mathrm{Int}\Big(L/2S_x + b \cdot \sin\frac{\pi}{3}\Big), \tag{6}$$

$$N_y = \mathrm{Int}(W/(2S_y + b). \tag{7}$$

In the expressions above, the term "Int" is an integer number function.

In this study, the energy equation (1) is solved numerically utilizing the finite-element technique. The corresponding variational statement has the following form[15]:

$$\begin{aligned} I_{\mathrm{n}} = \frac{1}{2}\iiint_{Ve} k\left(\frac{dT}{dx}\right)^2 dVe + \frac{1}{2}\iint_{A_{\mathrm{ps}}} h_{\mathrm{ps}}(T - T_\infty)^2 dA_{\mathrm{ps}} \\ + \frac{1}{2}\iint_{A_{\mathrm{pc}}} h_{\mathrm{pc}}(T - T_\infty)^2 dA_{\mathrm{pc}} + \iint_{A_{\mathrm{t}}} h_{\mathrm{t}}(T_{\mathrm{t}} - T_\infty)T dA_{\mathrm{t}}. \end{aligned} \tag{8}$$

The rationale for solving the heat transfer problem of a fin with triangular perforations may be best clarified by referring to Figs. 1–3. Figure 2 shows the symmetrical part considered for analysis (shown hatched). Figure 3 considers the part under study in detail, and shows the

existence of three regions (A, B, and C) around any perforation. In a sense, the regions A and C are uniform whereas the region B is tapered. The regions A and C are divided into $N_{\rm f}$ elements, respectively, while the region B is divided into $N_{\rm t}$ elements. The values of $N_{\rm f}$ and $N_{\rm t}$ are arbitrary according to the mesh generation requirements. The total number of elements $N_{\rm e}$ and the total number of nodes $N_{\rm n}$ are expressed as

$$N_{\rm e} = N_x(2N_{\rm f} + 2N_{\rm t}), \tag{9}$$

$$N_{\rm n} = N_{\rm e} + 1. \tag{10}$$

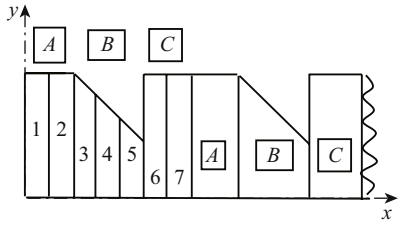

Fig. 3 Expanded symmetrical part with the three regions A, B and C considered in the mathematical formulation for the fin with triangular perforation (1, 2, 3, $\cdots$ are the numbers of the linear finite elements)

It is established that if everything else is the same, then the heat dissipation from a fin, whether solid or perforated, depends on the fin surface area and heat transfer coefficient. For the solid fin, both aspects are established. For a single horizontal plate under natural convection, the average value of $h_{\rm ss}$ may be given by[9]

$$h_{\rm ss} = Nu \cdot k_{\rm air}/Lc, \tag{11}$$

$$Lc = L \cdot W(2L + 2W). \tag{12}$$

The average Nusselt number, Nu, is given by[9]

$$Nu = (Nu_{\rm u} + Nu_{\rm l})/2, \tag{13}$$

$$Nu_{\rm u} = [(1.4/\ln(1 + 1.4/(0.43Ra^{0.25})))^{10} + (0.14Ra^{0.333})^{10}]^{0.1}, \tag{14}$$

$$Nu_{\rm l} = 0.527Ra^{0.2}/(1 + (1.9/Pr)^{0.9})^{2/9}, \tag{15}$$

where $10^6 < Ra < 10^8$.

For the fins considered in this study, both perforated and non-perforated, the fin tip is a vertical surface for which the Nusselt number $Nu_{\rm t}$ is given by[9]

$$Nu_t = 0.5\left(\left(\frac{2.8}{\ln\left(1 + \frac{2.8}{0.515\times Ra^{0.25}}\right)}\right)^6 + (0.103 \times Ra^{0.333})^6\right)^{\frac{1}{6}}, \tag{16}$$

$$h_{\rm t} = Nu_{\rm t} \cdot k_{\rm air}/Lc, \tag{17}$$

where $Lc = L \cdot t/(2L + 2t)$. As for the perforated fin, the aspect of its surface area was discussed in the previous section. However, three distinct heat transfer coefficients exist. The first one is the heat transfer coefficient of the solid portion of the perforated surface $h_{\rm ps}$, which can be calculated by the following expression[2]:

$$h_{\rm ps} = (1 + 0.75ROA) \cdot h_{\rm ss}, \tag{18}$$

$$ROA = \frac{OA}{OA_{\max}} = \frac{N_x \times N_y \times b^2 \times \sin\frac{\pi}{3}}{L \times W}. \tag{19}$$

The second one is the heat transfer coefficient within the perforation $h_{\rm pc}$. Its Nusselt number $Nu_{\rm c}$ is given by[9]

$$Nu_{\rm c} = \left[\left(\frac{Ra_{\rm c}}{13.3}\right)^{-\frac{3}{2}} + (0.62Ra_{\rm c}^{0.25})^{-1.5}\right]^{-\frac{2}{3}}, \tag{20}$$

$$Ra_{\rm c} = g \times \beta \times (T_{\rm m} - T_\infty) \times L_{\rm c}^4/(t \times \nu \times \mu), \tag{21}$$

$$L_{\rm c} = 2 \times A_{\rm c}/P_{\rm c}, \tag{22}$$

$$h_{\rm pc} = Nu_{\rm c} \times k_{\rm air}/L_{\rm c}, \tag{23}$$

where $Ra_{\rm c} < 10^4$.

The third one is that the heat transfer coefficient at fin tip $h_{\rm t}$, with its Nusselt number $Nu_{\rm t}$ given by Eqs. (16) and (17). The ratio of the heat dissipation of the perforated fin to that of the solid one RQF is introduced and given by

$$RQF = Q_{\rm pf}/Q_{\rm sf}, \tag{24}$$

where the heat dissipation of the perforated fin $Q_{\rm pf}$ is computed according to the finite element heat transfer solution described in Ref. [8]. The heat dissipation of the solid one ($Q_{\rm sf}$) is computed according to the exact solution described in Ref. [16].

3 Results and discussion

It is believed that comparing the perforated fin with its solid counterpart is the best means to evaluate improvement or non-improvement in heat transfer brought about by introducing the perforations. It is assumed that both fins have the same dimensions (the fin length is $L = 50$ mm and its width is $W = 100$ mm), same thermal conductivities, and same base and ambient temperatures, $T_{\rm b}$=100°C and T_∞=20°C. In this section, the findings are related to the temperature distribution along the fin or the heat transfer rate. The effect of introducing the perforations on these aspects is examined by comparing the perforated fin to its solid counterpart.

3.1 Temperature distribution $T(x)$

The temperature distribution along the perforated fin $T_{\rm pf}(x)$ is examined in terms of perforation parameters and fin thickness, where the perforation spacings are $S_x = S_y = 1$ mm. The temperature distribution along the fin length is plotted in Fig. 4. From the fin analysis literature, it is known that the high fin temperatures means high fin efficiency and effectiveness. Higher fin temperatures exist as long as low fin thermal conduction resistance exists. As indicated in Fig. 4, it is obvious that the temperature distributions show nonuniform curves caused by perforations. The perforations create a variation in the sectional area along the fin length and then lead to a variation in the fin thermal resistance. The variation effect of the perforated sectional area on its thermal resistance decreases as the thermal conductivity increases, so the curves become more uniform. To compare the temperature distribution of the perforated fin with that of the conventional (solid) one, the temperature difference distribution of the solid fin and the perforated fin $T_{\rm sf}(x) - T_{\rm pf}(x)$ is plotted in Fig. 5. As shown in the figure it is obvious that the temperatures along the solid (non-perforated) fin are always higher than those of the perforated one in all cases. This is because the thermal conduction resistance of the perforated fin is always higher than that of the corresponding non-perforated one. As the thermal conductivity increases, the difference $T_{\rm sf}(x) - T_{\rm pf}(x)$ decreases and approaches zero as the thermal conductivity approaches infinity. This is because as thermal conductivity approaches infinity, the fin (solid or perforated) becomes isothermal with the base temperature $T_{\rm b}$. Figures 4 and 5 show that the temperature difference (temperature drop) between the fin base and its

tip increases as the triangular perforation dimension b increases. This is because the thermal resistance of the perforated fin increases as b increases. Consequently, from the viewpoint of a temperature distribution, it is recommended to use small perforation dimensions as much as possible. Also, it can be deduced from the temperature distribution that the fin temperatures increase as the fin thickness increases. This is readily explained by the fact that the thermal resistance of the perforated fin decreases as the fin thickness increases. Therefore, from the temperature distribution viewpoint, it is preferable to use large fin thicknesses as possible. The curves in Figs. 4 and 5 are zigzag due to the fact that there is a significant variation in the thermal resistance along the length of the perforated fin. It is obvious that this thermal resistance increases in the regions adjacent to the perforation. Also, this resistance increases as the solid sectional area of the perforated fin decreases. The variation in this thermal resistance leads to a variable slope of the temperature distribution curves.

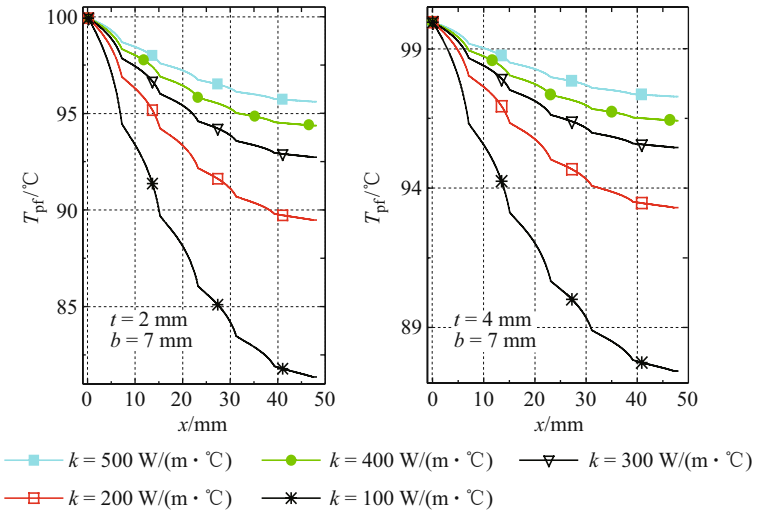

Fig. 4 Temperature distribution along the length of the perforated fin with variable fin thickness and perforation dimension

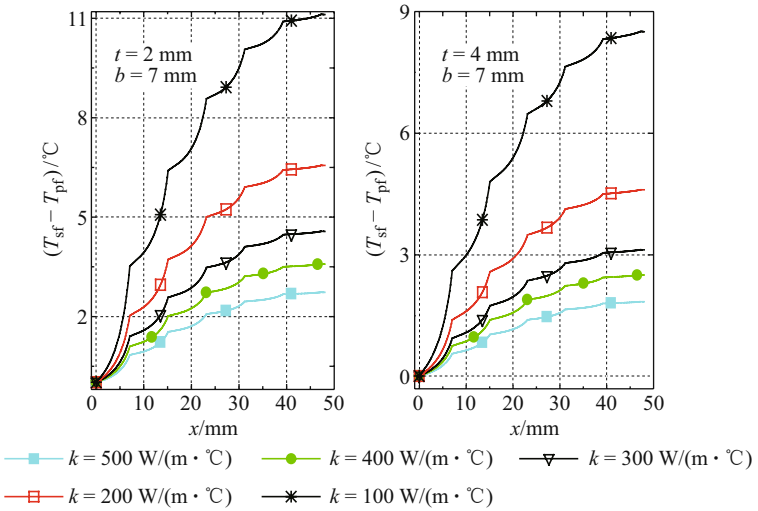

Fig. 5 Temperature difference distribution along the length of the perforated fin with variable fin thickness and perforation dimension

3.2 Ratio of heat dissipation rate (RQF)

The ratio of the heat dissipation rate from the perforated fin to that of the corresponding solid fin, RQF, is studied in terms of the perforation dimension b for different values of fin thickness. The results are shown in Fig. 6, which shows that thicker fins produce larger heat transfer enhancement at any b. The variations of RQF with b at various thicknesses t show a consistent trend of increasing to a maximum followed by a decrease. This trend may be explained by the net effects of change in fin heat transfer surface area and heat transfer coefficients due to the perforations. Furthermore, the figure shows that RQF is a strong function of the perforation dimension b and the fin thickness. The perforation dimension at which the RQF ratio has a maximum value, is referred to as the optimum perforation dimension b_o. Figure 6 indicates that the optimum dimension b_o is a strong function of the fin thickness. The approximate values of b_o can be obtained from the curves shown in Fig. 6. These values are arranged in Table 1.

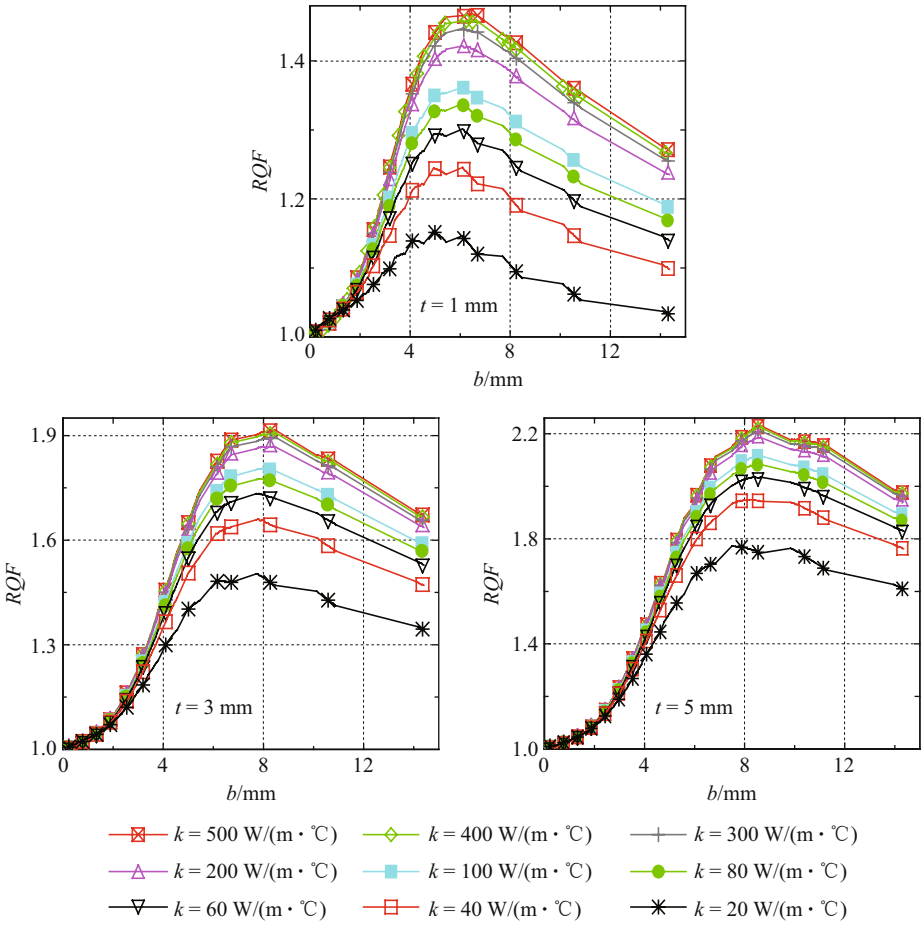

Fig. 6 Ratio of heat dissipation rate RQF vs. perforation dimension with variable fin thickness and thermal conductivity

Table 1 Approximate values of the optimum perforation diameter of the perforated fin

Fin thickness/mm	1	2	3	4	5
Optimum dimension b_o/mm	5.8	6.7	7.5	8.1	8.5

To investigate the effect of the longitudinal spacing S_x on the perforated fin performance, the heat dissipation ratio RQF is plotted as a function of the spacing S_x, as shown in Fig. 7. The figure indicates that at any t, RQF decreases with an increase in spacing S_x. This behavior is due to the fact that an increasing S_x means a smaller number of perforations. This means the loss of the element causes the heat transfer enhancement. Therefore, according to S_x spacing it is preferable to minimize it as possible. The effect of lateral spacing S_y on the perforated fin performance can be investigated by plotting RQF as a function of S_y for various thermal conductivities as shown in Fig. 8. The figure shows that RQF increases in the low values of S_y and then tends to decline thereafter. It may be suggested here that the conflicting effects of the fin thermal resistance and the number of perforations are responsible for this trend. Figure 7 shows that RQF heavily depends on the spacing S_y. The figure indicates that RQF values which are closely related to the optimum perforation dimension b_o, are strong functions of the spacing S_y. In this region, the ratio RQF attains a maximum value and then decreases as the spacing S_y increases. This means that there is an optimum associated value of the spacing S_y, which is abbreviated as S_{yo}. The values of S_{yo} strongly depend on the fin thickness and its thermal conductivity. The approximate values of S_{yo} can be obtained from the curves shown in Fig. 8. The approximate values of S_{yo} are plotted in Fig. 9. This figure shows that S_{yo} decreases as fin thermal conductivity and thickness increase. To summarize the advantages of

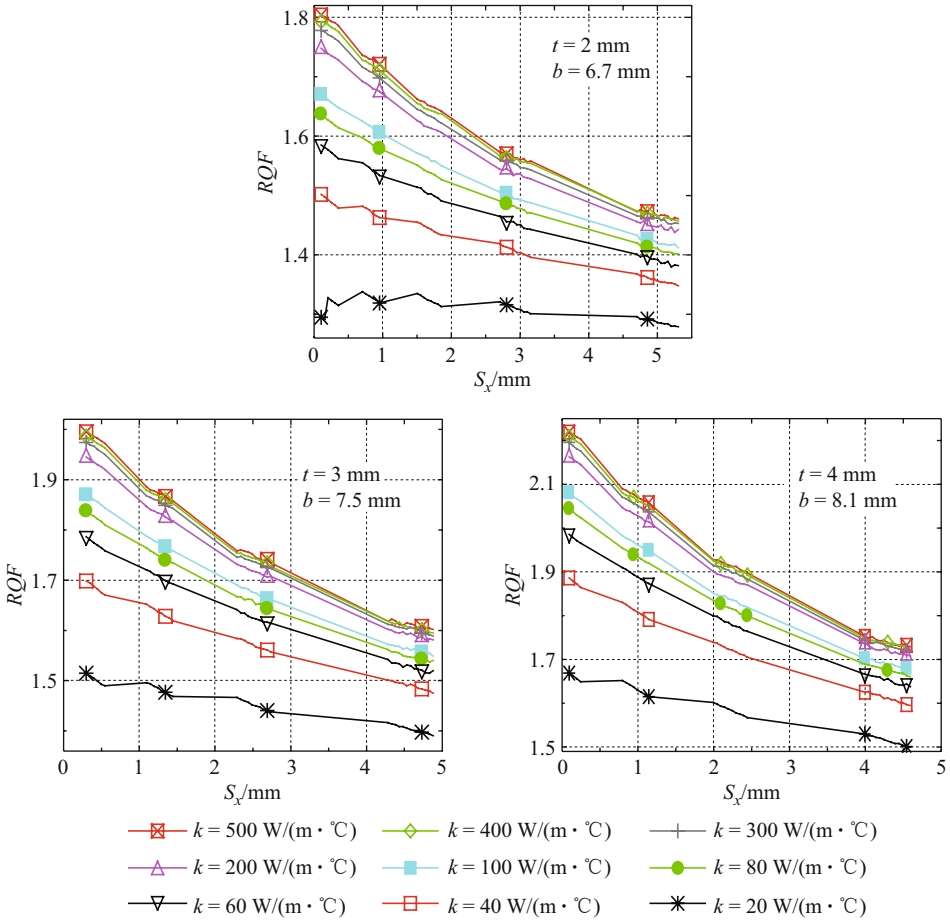

Fig. 7 Ratio of heat dissipation rate RQF vs. longitudinal spacing S_x with variable fin thickness and thermal conductivity

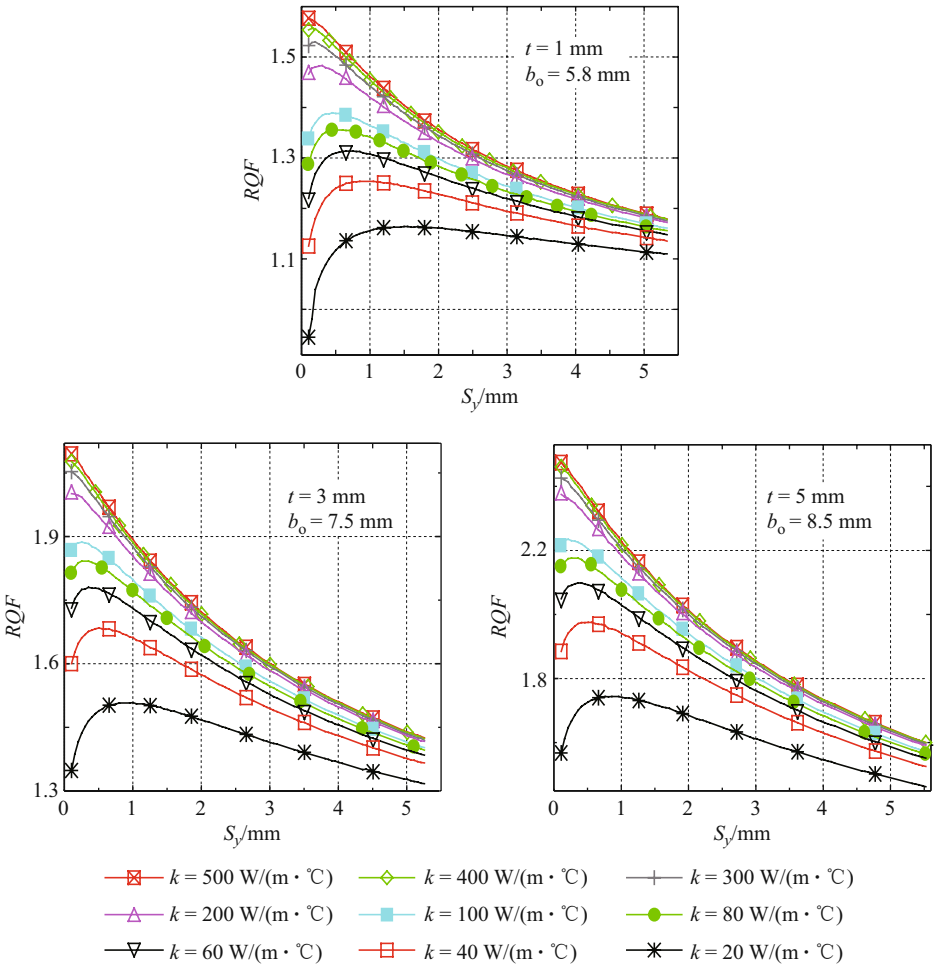

Fig. 8 Ratio of heat dissipation rate RQF vs. lateral spacing S_y with variable fin thickness for low and high thermal conductivities

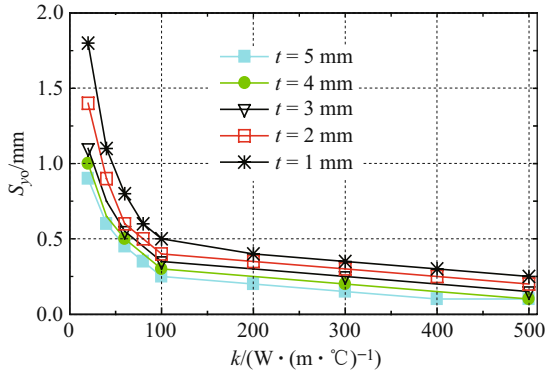

Fig. 9 Optimum lateral spacing S_{yo} vs. thermal conductivity of the perforated fin at varying thickness

using the perforated fin at the optimum values of perforation geometry, the ratios of heat dissipation RQF and of weight reduction RWF are plotted as functions of the fin thickness with variable fin thermal conductivity at the optimum perforation diameter b_o and optimum lateral spacing S_{yo} as shown in Fig. 10. Figure 10 shows that the use of perforations in fins leads to the enhanced heat dissipation and decreased fin weight. The enhancement is increased and the weight reduction decreases as the fin thickness and thermal conductivity increase. This means that the use of a perforated fin leads to enhanced heat dissipation rates and at the same time leads to the decreased expenditure for fin materials.

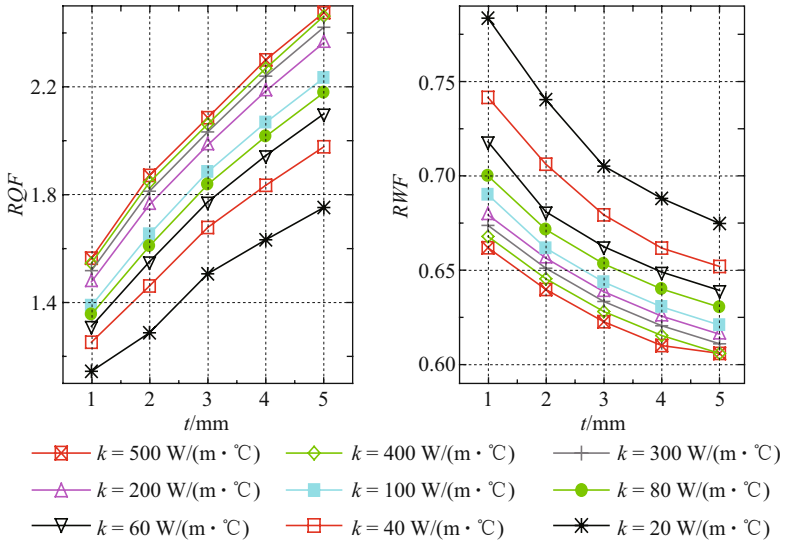

Fig. 10 Ratio of heat dissipation rate RQF and ratio of reduction weight RWF vs. fin thickness with variable fin thermal conductivity at the optimum perforation dimension b_o and optimum lateral spacing S_{yo}

4 Conclusions

(i) The temperature drop along the perforated fin length is consistently larger than that on an equivalent non-perforated fin.

(ii) For certain values of triangular dimensions, the perforated fin can enhance heat transfer. The magnitude of enhancement is proportional to the fin thickness and its thermal conductivity.

(iii) The extent of the heat dissipation rate enhancement for perforated fins is a complicated function of the fin dimensions, the perforation geometry and the fin thermophysical properties.

(iv) The gain in the heat dissipation rate for the perforated fin is a strong function of both the perforation diameter and lateral spacing. This function attains a maximum value at a given perforation diameter and spacing, which are called the optimum perforation dimension b_o, and the optimum spacing S_{yo}, respectively.

(v) The perforation of fins enhances the heat dissipation rates and at the same time decreases the expenditure for fin materials.

References

[1] Bergles A E. Technique to augment heat transfer[M]. 2nd Ed. In: Werren M Rohsenow, James P Hartnett, Ejup N Ganic (eds). *Handbook of Heat Transfer Applications*, Ch.3, New York: McGraw-Hill Book Company, 1985.

[2] Al-Essa A H, Al-Hussien F M S. The effect of orientation of square perforations on the heat transfer enhancement from a fin subjected to natural convection[J]. *Heat and Mass Transfer*, 2004, **40**:509–515.

[3] Mullisen R, Loehrke R. A study of flow mechanisms responsible for heat transfer enhancement in interrupted-plate heat exchangers[J]. *Journal of Heat Transfer* (*Transactions of the ASME*), 1986, **108**:377–385.

[4] Prasad B V S S S, Gupta A V S S K S. Note on the performance of an optimal straight rectangular fin with a semicircular cut at the tip[J]. *Heat Transfer Engineering*, 1998, **14**(1):53–57.

[5] Kutscher C F. Heat exchange effectiveness and pressure drop for air flow through perforated plates with and without crosswind[J]. *Journal of Heat Transfer*, 1994, **116**:391–399.

[6] Chung B T F, Iyer J R. Optimum design of longitudinal rectangular fins and cylindrical spines with variable heat transfer coefficient[J]. *Heat Transfer Engineering*, 1993, **14**(1):31–42.

[7] Kakac S, Bergles A E, Mayinger F. Heat exchangers, thermal-hydraulic fundamentals and design[M]. Washington, DC: Hemisphere Publishing Corporation, 1981.

[8] Al-Essa A H. Enhancement of thermal performance of fins subjected to natural convection through body perforation[D]. Ph D dissertation. Department of Mechanical Engineering, University of Baghdad, Iraq and University of Science and Technology, Jordan. 2000.

[9] Raithby G D, Holands K G T. Natural convection[M]. 2nd Ed. In: Rohsenow W, Hartnett J, Ganic E (eds). *Handbook of Heat Transfer Applications*, Ch. 6, New York: McGraw-Hill Book Company, 1984.

[10] Sparrow E M, Oritz M Carranco. Heat transfer coefficient for the upstream face of a perforated plate positioned normal to an oncoming flow[J]. *Int J Heat Mass Transfer*, 1982, **25**(1):127–135.

[11] Ugur Akyol, Kadir Bilen. Heat transfer and thermal performance analysis of a surface with hollow rectangular fins[J]. *Applied Thermal Engineering*, 2006, **26**:209–216.

[12] Bayram Sahin, Alparslan Demir. Performance analysis of a heat exchanger having perforated square fins[J]. *Applied Thermal Engineering*, 2008, **28**(5/6):621–623.

[13] Aziz A, Lunadini V. Multidimensional steady conduction in convicting, radiating, and convicting-radiating fins and fin assemblies[J]. *Heat Transfer Engineering*, 1995, **16**(3):32–64.

[14] Razelos P, Georgiou E. Two-dimensional effects and design criteria for convective extended surfaces[J]. *Heat Transfer Engineering*, 1992, **13**(3):38–48.

[15] Rao S S. The finite element method in engineering[M]. 2nd Ed. Elmsford, New York: Pergamon, 1989.

[16] Incropera Frank P, Dewitt David P. Fundamentals of heat and mass transfer[M]. 4th Ed. New York: John Wiley and Sons 1996, p110.